

Nonlinear Flight Control in the Presence of Structural Changes and External Disturbances

Vahram Stepanyan and Andrew Kurdila

Abstract—This paper presents a flight control design methodology for the full nonlinear model of unmanned aerial vehicles in the presence of parametric and nonparametric modeling uncertainties and unknown external disturbances. The proposed controller is based on function approximations, adaptive block backstepping and continuous adaptive bounding techniques. It guarantees asymptotic tracking of a given smooth reference command and stability of the closed-loop system, assuming no knowledge on the bounds of uncertainties. The performance of the control algorithm is demonstrated on a simulation example.

I. INTRODUCTION

Recent years have witnessed increasing involvement of unmanned aerial vehicles (UAV) in many military and civilian operations. In cases, when the presence of human operators is not desirable or is dangerous, the automatic flight control system determines the success of the mission. Therefore, the development of reliable control systems that can compensate for uncertain flight conditions is imperative.

The existing methods mainly are based on neural network approximations of unknown functions and typically achieve only ultimate bounded tracking due to inherent function reconstruction error (see for example Refs. [2], [13], [14], [21]). Also, since the NN weights estimates update laws are defined based on a Lyapunov function, the time derivative of which is usually shown to be only positive semi-definite outside a compact region independent of the weight estimation errors, the weight estimates can drift to infinity unless some special care is taken. Some modifications include the projection based adaptive laws [19], e -modification [6], σ -modification [15] or dead-zone technique [10].

When the unknown functions' bounds are available, robust control methods, such as a sliding mode control can be used to achieve an asymptotic tracking (see for example [8], [3]). However, these controllers are usually discontinuous and generate chattering, which is undesirable in most of the applications. It can be avoided higher order sliding mode control [1], [12], [23]. However, this approach requires the knowledge of not only the bound of uncertain functions, but also of their derivatives. The alternative approach with the similar assumptions is presented in [25].

This material is based upon work supported by Office of Naval Research under Contract No N00014-06-1-0801.

V.Stepanyan is with Department of Mechanical Engineering, Virginia Polytechnic Institute and State University, Blacksburg, VA 24061, USA vahrams@vt.edu

V.Stepanyan is with Department of Mechanical Engineering, Virginia Polytechnic Institute and State University, Blacksburg, VA 24061, USA kurdila@vt.edu

In this paper we use the adaptive bounding technique, originally introduced in [18] and developed in [5], in conjunction with the error filtering and block-backstepping [11] to design a continuous flight control for the nonlinear model of a UAV that is subject to parametric uncertainties, resulting from the actuator failures and structural damages, modeling uncertainties and external disturbances. The proposed robust adaptive controller achieves asymptotic tracking of the given smooth reference commands and stability of the closed-loop system under the mild assumptions of the smoothness of the uncertainties and absolute continuity of external disturbances. However, no knowledge of the bounds is assumed. Meantime, the resulting control signals are of low frequency.

The rest of the paper is organized as follows. In Section II we present the model dynamic, discuss the problem statement, define the control objective and give the error dynamics. The control architecture is presented in Section III. Section IV represents the stability analysis. The simulation results are presented in Section V. Throughout the manuscript bold symbols denote the vector quantities.

II. PROBLEM FORMULATION

A. Aircraft Model

Consider the dynamic equations of the aircraft written in combined wind and body axis [24] subject to external disturbances $d_0(t)$ and $\mathbf{d}(t) = [d_1(t) \ d_2(t) \ d_3(t)]^\top$ representing the unknown atmospheric effects:

$$\begin{aligned} \dot{V}_T(t) &= \frac{T}{m} \cos \beta(t) \cos \alpha(t) - \frac{D}{m} - g \sin \gamma(t) + \frac{d_0(t)}{m} \\ \dot{\alpha}(t) &= q(t) - p(t) \cos \alpha(t) \tan \beta(t) \\ &\quad - r(t) \sin \alpha(t) \tan \beta(t) - q_w(t) \sec \beta(t) \\ \dot{\beta}(t) &= r_w(t) + p(t) \sin \alpha(t) - r(t) \cos \alpha(t) \\ \dot{\mathbf{E}}(t) &= \mathbf{R}(t)\boldsymbol{\omega}(t) \\ \dot{\boldsymbol{\omega}}(t) &= \mathbf{J}^{-1} [-\boldsymbol{\omega}(t) \times \mathbf{J}\boldsymbol{\omega}(t) + \mathbf{M} + \mathbf{d}(t)] \end{aligned} \quad (1)$$

where $\mathbf{E} = [\phi \ \theta \ \psi]^\top$, $\boldsymbol{\omega} = [p \ q \ r]^\top$, $\mathbf{M} = [\mathcal{L} \ \mathcal{M} \ \mathcal{N}]^\top$, $q_w = \frac{1}{mV_T}[L - mg \cos \mu \cos \gamma + T \sin \alpha]$, $r_w = \frac{1}{mV_T}[Y + mg \sin \mu \cos \gamma - T \sin \beta \cos \alpha]$, \mathbf{J} is the inertia matrix assuming to be diagonal (that is the body frame is chosen as close to the principal frame as possible in order the cross-inertia terms to be negligible) and

$$\mathbf{R}(t) = \begin{bmatrix} 1 & \sin \phi(t) \tan \theta(t) & \cos \phi(t) \tan \theta(t) \\ 0 & \cos \phi(t) & -\sin \phi(t) \\ 0 & \sin \phi(t) \sec \theta(t) & \cos \phi(t) \sec \theta(t) \end{bmatrix}.$$

It is assumed that the thrust and aerodynamic moments are linear in corresponding control surface deflections and can

be expressed in following form:

$$T = T_{\delta_T} \delta_T + \Delta_T(\mathbf{x}), \quad \mathcal{L} = \mathcal{L}_{\delta_a} \delta_a + \mathcal{L}_{\delta_r} \delta_r + \Delta_{\mathcal{L}}(\mathbf{x})$$

$$\mathcal{M} = \mathcal{M}_{\delta_e} \delta_e + \Delta_{\mathcal{M}}(\mathbf{x}), \quad \mathcal{N} = \mathcal{N}_{\delta_a} \delta_a + \mathcal{N}_{\delta_r} \delta_r + \Delta_{\mathcal{N}}(\mathbf{x}),$$

where $\Delta_T(\mathbf{x})$, $\Delta_{\mathcal{L}}(\mathbf{x})$, $\Delta_{\mathcal{M}}(\mathbf{x})$, $\Delta_{\mathcal{N}}(\mathbf{x})$ represent the remaining parts of the actual thrust and aerodynamic moments that are assumed to be continuously differentiable unknown functions of the states $\mathbf{x} = [V \ \alpha \ \beta \ \boldsymbol{\omega}^\top]^\top$ of the system (1), in some compact domain of possible initial conditions $\Omega_{\mathbf{x}}$.

B. Control Objective

The control objective is to design control surface deflection commands $\delta_T(t)$, $\delta_a(t)$, $\delta_e(t)$, $\delta_r(t)$ such that the aircraft's airspeed and the orientation angles asymptotically track without sideslip the desired reference commands $V_c(t)$, $\phi_c(t)$, $\theta_c(t)$, $\psi_c(t)$ in the presence of modeling uncertainties $\Delta_T(\mathbf{x})$, $D(\mathbf{x})$, $\Delta_{\mathcal{L}}(\mathbf{x})$, $\Delta_{\mathcal{M}}(\mathbf{x})$, $\Delta_{\mathcal{N}}(\mathbf{x})$ and external disturbances $d_0(t)$, $\mathbf{d}(t)$, which are assumed to be absolutely continuous bounded functions of time.

We further assume that the reference commands are sufficiently smooth, otherwise the pre-filters are used to achieve the required smoothness. Specifically, we assume that $V_c(t) \in \underline{\mathcal{L}}_\infty \cap C^{(2)}$, $\dot{V}_c(t) \in \mathcal{L}_\infty$, $\phi_c(t)$, $\theta_c(t)$, $\psi_c(t) \in \mathcal{L}_\infty \cap C^{(3)}$, $\dot{\phi}_c(t)$, $\ddot{\theta}_c(t)$, $\dot{\psi}_c(t) \in \mathcal{L}_\infty$.

C. Effects of Structural Changes

The unknown structural changes alter the aircraft's mass, inertia, propulsion and aerodynamic forces and moments. We assume that the aerodynamic effects of the structural changes are accounted in the modeling uncertainties $\Delta_T(\mathbf{x})$, $\Delta_D(\mathbf{x})$, $\Delta_{\mathcal{L}}(\mathbf{x})$, $\Delta_{\mathcal{M}}(\mathbf{x})$, $\Delta_{\mathcal{N}}(\mathbf{x})$. However, the structural changes that affect the control effectiveness must be taken into account explicitly. That is, we assume that these changes result in unknown positive coefficients $\lambda_i^* \leq \lambda_i \leq 1$, $i = T, a, e, r$ for the thrust and moments generated by the control surface deflections δ_T , δ_a , δ_e , δ_r respectively. Here the constants λ_i^* , $i = T, a, e, r$ represent the lower bounds, beyond which the UAV practically loses the controllability. Thus the aircraft's dynamics equations (without the internal dynamics) can be written as

$$\begin{aligned} \dot{V}_T(t) &= b^{-1}u(t) - g \sin \gamma(t) + f(\mathbf{x}) + d_0(t) \\ \dot{\mathbf{E}}(t) &= R(t)\boldsymbol{\omega}(t) \\ \dot{\boldsymbol{\omega}}(t) &= B^{-1}\boldsymbol{\delta}(t) + \mathbf{F}(\mathbf{x}) + \mathbf{d}(t), \end{aligned} \quad (2)$$

where m and J are the unknown values of the UAV mass and inertia matrix respectively, and the following notations are introduced: $u(t) = T_{\delta_T} \cos \beta(t) \cos \alpha(t) \delta_T(t)$, $b^{-1} = \frac{\lambda_T}{m}$, $d_0(t) \triangleq \frac{1}{m}d_0(t)$, $f(\mathbf{x}) = \frac{1}{m}[-D(\mathbf{x}) + \Delta_T(\mathbf{x}) \cos \beta(t) \cos \alpha(t)]$, $B = \Lambda^{-1}J$, $\mathbf{F}(\mathbf{x}) = J^{-1}[-\boldsymbol{\omega} \times J\boldsymbol{\omega} + \Delta_{\mathcal{M}}(\mathbf{x})]$, $\mathbf{d}(t) \triangleq J^{-1}\mathbf{d}(t)$, $\boldsymbol{\delta} = B_0[\delta_a \ \delta_e \ \delta_r]^\top$, $\Delta_{\mathcal{M}} = [\Delta_{\mathcal{L}} \ \Delta_{\mathcal{M}} \ \Delta_{\mathcal{N}}]^\top$, and

$$B_0 = \begin{bmatrix} \mathcal{L}_{\delta_a} & 0 & \mathcal{L}_{\delta_r} \\ 0 & \mathcal{M}_{\delta_e} & 0 \\ \mathcal{N}_{\delta_a} & 0 & \mathcal{N}_{\delta_r} \end{bmatrix}, \quad \Lambda = \begin{bmatrix} \lambda_a & 0 & 0 \\ 0 & \lambda_e & 0 \\ 0 & 0 & \lambda_r \end{bmatrix}.$$

We notice that the parameters m and J satisfy the bounds $m_* \leq m \leq m^*$ and $J_* \leq J \leq J^*$, where m_* and J_* are the lower practical limit for the mass and inertia matrix. (Recall that for the matrices $A \geq B$ means that $A - B$ is positive semi-definite.) Also, the unknown matrix B is diagonal and positive definite, and the matrix B_0 is normally invertible, hence the control surface deflections can be determined from the equation $[\delta_a \ \delta_e \ \delta_r]^\top = B_0^{-1}\boldsymbol{\delta}$ after $\boldsymbol{\delta}$ is designed.

D. Error Dynamics

We introduce the tracking errors as follows

$$\begin{aligned} \tilde{V}(t) &= V_T(t) - V_c(t), \quad \tilde{\phi}(t) = \phi(t) - \phi_c(t) \\ \tilde{\theta}(t) &= \theta(t) - \theta_c(t), \quad \tilde{\psi}(t) = \psi(t) - \psi_c(t). \end{aligned} \quad (3)$$

Corresponding error dynamics are written as

$$\begin{aligned} \dot{\tilde{V}}(t) &= b^{-1}u(t) - g \sin \gamma(t) + f(\mathbf{x}) + d(t) - \dot{V}_c(t) \\ \dot{\tilde{\mathbf{E}}}(t) &= R(t)\boldsymbol{\omega}(t) - \dot{\mathbf{E}}_c(t) \end{aligned} \quad (4)$$

where $\tilde{\mathbf{E}} = [\tilde{\phi} \ \tilde{\theta} \ \tilde{\psi}]^\top$. The error dynamics for the angular rates are derived using block-backstepping technique [11]. To this end we define a virtual control $\boldsymbol{\omega}_c(t) = \bar{R}(t)[-K_1\tilde{\mathbf{E}}(t) + \dot{\mathbf{E}}_c(t)]$ that stabilizes the $\tilde{\mathbf{E}}$ -dynamics in (4). Here $K_1 > 0$ is the desired time constants for the orientation angle dynamics and the matrix $\bar{R}(t)$ is given by

$$\bar{R}(t) = \begin{bmatrix} 1 & 0 & -\sin \theta(t) \\ 0 & \cos \phi(t) & \sin \phi(t) \cos \theta(t) \\ 0 & -\sin \phi(t) & \cos \phi(t) \cos \theta(t) \end{bmatrix}.$$

Defining the angular rate error as $\tilde{\boldsymbol{\omega}}(t) = \boldsymbol{\omega}(t) - \boldsymbol{\omega}_c(t)$, the error dynamics can be expressed as

$$\begin{aligned} \dot{\tilde{V}}(t) &= b^{-1}u(t) - g \sin \gamma(t) + f(\mathbf{x}) + d_0(t) - \dot{V}_c(t) \\ \dot{\tilde{\mathbf{E}}}(t) &= R(t)\tilde{\boldsymbol{\omega}}(t) - K_1\tilde{\mathbf{E}}(t) \\ \dot{\tilde{\boldsymbol{\omega}}}(t) &= B^{-1}\boldsymbol{\delta}(t) + \mathbf{F}(\mathbf{x}) + \mathbf{d}(t) - \dot{\boldsymbol{\omega}}_c(t). \end{aligned} \quad (5)$$

To complete the error dynamics we introduce the desired values for the sideslip angle and angle of attack. The desired sideslip angle is $\beta_c = 0$, therefore the error in sideslip is $\tilde{\beta}(t) = \beta(t)$. The desired angle of attack is chosen to be a trim value α_e , corresponding to a trim velocity V_e from the operating range of $V_c(t)$. Then the error is $\tilde{\alpha}(t) = \alpha(t) - \alpha_e$. The respective error dynamics are given as

$$\dot{\tilde{\beta}}(t) = r_w(t) + p(t) \sin \alpha(t) - r(t) \cos \alpha(t) \quad (6)$$

$$\begin{aligned} \dot{\tilde{\alpha}}(t) &= q(t) - p(t) \cos \alpha(t) \tan \beta(t) \\ &\quad - r(t) \sin \alpha(t) \tan \beta(t) - q_w(t) \sec \beta(t) \end{aligned} \quad (7)$$

The control objective is reduced to the stabilization of the error dynamics by the choice of control inputs $u(t)$ and $\boldsymbol{\delta}(t)$.

E. Internal Dynamics

The system in (1) has relative degree one with respect to the output $V_T(t)$ and relative two with respect to the outputs $\phi(t)$, $\theta(t)$, $\psi(t)$. This implies that the system has second order internal dynamics consisting of the α and β dynamics, which are not controlled directly. This can be

motivated by the fact that the control surfaces are primarily moment generators, that is the dependencies of drug, lift and side forces on the control surface deflections are negligible. The zero dynamics can be viewed as a perturbation from the trim straight flight with constant parameters V_e , α_e , θ_e . The stability of the zero dynamics is established by setting $V_T(t) = V_e$, $p = q = r = 0$ and $\phi = 0$ in the α and β dynamics, which results in

$$\begin{aligned}\dot{\tilde{\alpha}}(t) &= -\frac{\sec \beta(t)}{mV_T} [L(\alpha) - L_e + T \sin \alpha(t) - T \sin \alpha_e] \\ \dot{\tilde{\beta}}(t) &= \frac{1}{mV_T} [Y(\beta) - T \cos \alpha(t) \sin \beta(t)],\end{aligned}\quad (8)$$

where $\tilde{\alpha}(t) = \alpha(t) - \alpha_e$, $\tilde{\beta}(t) = \beta(t)$, ($\beta_e = 0$). Applying the mean value theorem to the $\tilde{\alpha}$ dynamics we obtain $\tilde{L}(\alpha) = L(\alpha) - L_e = S\bar{q}C_L(\alpha^*)\tilde{\alpha}$ and $\tilde{T}(\alpha) = T \sin \alpha(t) - T \sin \alpha_e = T \cos(\alpha^*)\tilde{\alpha}$. Assuming that $T > 0$, $C_L(\alpha) > 0$ and $\beta Y(\beta) < 0$, which is the case for the conventional aircraft, it follows that the zero-dynamics are exponentially stable on the square $S_0 = \{(\tilde{\alpha}, \tilde{\beta}) : -\pi/2 < \tilde{\alpha}, \tilde{\beta} < \pi/2\}$. It can be shown that for the internal dynamics the derivative of the positive definite function

$$V_0(t) = \frac{1}{2}[\tilde{\alpha}^2(t) + \tilde{\beta}^2(t)],\quad (9)$$

satisfies the following inequality

$$\dot{V}_0(t) \leq -c_0[\tilde{\alpha}^2(t) + \tilde{\beta}^2(t)] + c_1 [\|\tilde{\omega}(t)\|^2 + \tilde{V}^2(t)],\quad (10)$$

where c_1 is a positive constant.

III. CONTROL DESIGN

In this section we give the control system architecture, which has the advantage to generate low frequency control signals and to meet the control objective.

A. Airspeed Control

First we design the stabilizing controller for the airspeed error dynamics by introducing the auxiliary variable

$$\eta(t) = k\tilde{V}(t) + \dot{\tilde{V}}(t),\quad (11)$$

the dynamics of which can be expressed as follows:

$$b\dot{\eta}(t) = \bar{u}(t) + g_0(\mathbf{x}(t), \dot{\mathbf{x}}(t)) + h_0(t),\quad (12)$$

where $k > 0$ is a design constant, $\bar{u}(t) = G_0(s)u(t)$ is the new control, $G_0(s) = s + k$ is a differential operator, and

$$\begin{aligned}g_0(\mathbf{x}(t), \dot{\mathbf{x}}(t)) &= bG_0(s) [f(\mathbf{x}(t)) - g \sin \gamma(t)] \\ h_0(t) &= bG_0(s)[d_0(t) - \dot{V}_c(t)],\end{aligned}\quad (13)$$

We notice that $h_0(t)$ is uniformly bounded, and $g_0(\mathbf{x}, \dot{\mathbf{x}})$ is continuous in \mathbf{x} and $\dot{\mathbf{x}}$. Therefore it can be approximated over a compact domain $\Omega_x \times \Omega_{\dot{x}}$ by a linear in parameters radial basis function (RBF) neural network [17]:

$$g_0(\mathbf{x}, \dot{\mathbf{x}}) = \mathbf{w}^\top \boldsymbol{\varphi}(\mathbf{x}, \dot{\mathbf{x}}) + \epsilon_0(\mathbf{x}, \dot{\mathbf{x}}),\quad (14)$$

where $\mathbf{w} \in \mathbb{R}^N$ is the vector of unknown constant parameters to be estimated online, and $\boldsymbol{\varphi}(\mathbf{x}, \dot{\mathbf{x}})$ is the vector of RBFs,

and $\epsilon_0(\mathbf{x}, \dot{\mathbf{x}})$ is the uniformly bounded reconstruction error. The airspeed error equation can be now written as

$$\begin{aligned}\dot{\tilde{V}}(t) &= -k\tilde{V}(t) + \eta(t) \\ b\dot{\eta}(t) &= \bar{u}(t) + \mathbf{w}^\top \boldsymbol{\varphi}(\mathbf{x}_c, \dot{\mathbf{x}}_c) + \sigma_0(t),\end{aligned}\quad (15)$$

where the uniformly bounded function $\sigma_0(t)$ has the form

$$\sigma_0(t) = h_0(t) + \epsilon_0(\mathbf{x}, \dot{\mathbf{x}}) + \mathbf{w}^\top [\boldsymbol{\varphi}(\mathbf{x}, \dot{\mathbf{x}}) - \boldsymbol{\varphi}(\mathbf{x}_c, \dot{\mathbf{x}}_c)].$$

The control signal is defined according to equation

$$\bar{u}(t) = -\tilde{V}(t) - c\eta(t) - \hat{\mathbf{w}}^\top \boldsymbol{\varphi}(\mathbf{x}_c, \dot{\mathbf{x}}_c) - \hat{\sigma}_0(t)\text{sign}(\tilde{V}(t)),$$

where $c > 0$ is the design parameter, $\hat{\mathbf{w}}$ is the estimate of the unknown weight \mathbf{w} , and $\hat{\sigma}_0(t)$ is the estimate of the unknown upper bound σ_0^* of $\sigma_0(t)$. The airspeed control architecture is concluded by the adaptive laws for the estimates $\hat{\sigma}_0(t)$ and $\hat{\mathbf{w}}(t)$ given as

$$\begin{aligned}\dot{\hat{\sigma}}_0(t) &= \mu_0\eta(t)\text{sign}(\tilde{V}(t)) \\ \dot{\hat{\mathbf{w}}}(t) &= \Gamma_0\eta(t)\boldsymbol{\varphi}(\mathbf{x}_c, \dot{\mathbf{x}}_c),\end{aligned}\quad (16)$$

where μ_0 and Γ_0 are the adaptation gains. The actual control signal is the output of the low pass filter

$$u(t) = \frac{1}{s+k}\bar{u}(t).\quad (17)$$

The resulting airspeed error dynamics take the form

$$\begin{aligned}\dot{\tilde{V}}(t) &= -k\tilde{V}(t) + \eta(t) \\ b\dot{\eta}(t) &= -\tilde{V}(t) - c\eta(t) - \hat{\mathbf{w}}^\top \boldsymbol{\varphi}(\mathbf{x}_c, \dot{\mathbf{x}}_c) \\ &\quad - \hat{\sigma}_0(t)\text{sign}(\tilde{V}(t)) + \sigma_0(t),\end{aligned}\quad (18)$$

B. Orientation Control

The design of the orientation control $\delta(t)$ essentially follows the same steps as in the case of the airspeed control. The main difference is that the backstepping error term $R(t)\tilde{\mathbf{E}}(t)$ has to be included in the expression of the auxiliary variable

$$\zeta(t) = K_2\tilde{\omega}(t) + \dot{\tilde{\omega}}(t) + R(t)\tilde{\mathbf{E}}(t),\quad (19)$$

where K_2 is a positive definite gain matrix. The orientation error dynamics take the form

$$\begin{aligned}\dot{\tilde{\mathbf{E}}}(t) &= R(t)\tilde{\omega}(t) - K_1\tilde{\mathbf{E}}(t) \\ \dot{\tilde{\omega}}(t) &= \zeta(t) - K_2\tilde{\omega}(t) - R(t)\tilde{\mathbf{E}}(t) \\ B\dot{\zeta}(t) &= \bar{\delta}(t) + \mathbf{g}(\mathbf{x}, \mathbf{x}_c) + B\mathbf{a}(\mathbf{E}, \boldsymbol{\omega}, \tilde{\mathbf{E}}, \tilde{\omega}) + \mathbf{h}(t),\end{aligned}\quad (20)$$

where $\bar{\delta}(t) = G(s)\delta(t)$ is the new control input, $G(s) = s\mathbb{I} + K_2$ is a matrix differential operator, $\mathbf{g}(\mathbf{x}, \mathbf{x}_c) = BG(s)\mathbf{F}(\mathbf{x}_c(t))$, $\mathbf{h}(t) = BG(s)[\mathbf{d}(t) - \dot{\boldsymbol{\omega}}_c(t)]$ and $\mathbf{a}(\mathbf{E}, \boldsymbol{\omega}, \tilde{\mathbf{E}}, \tilde{\omega}) = \frac{d}{dt}R(t)\tilde{\mathbf{E}}(t)$. We notice that $\mathbf{h}(t)$ is uniformly bounded, and $\mathbf{g}(\mathbf{x}, \dot{\mathbf{x}})$ is continuous in \mathbf{x} and $\dot{\mathbf{x}}$. Therefore it can be approximated over a compact domain $\Omega_x \times \Omega_{\dot{x}}$ by a linear in parameters radial basis function (RBF) neural network [17]:

$$\mathbf{g}(\mathbf{x}, \dot{\mathbf{x}}) = W_1^\top \boldsymbol{\varphi}(\mathbf{x}, \dot{\mathbf{x}}) + \epsilon_1(\mathbf{x}, \dot{\mathbf{x}}),\quad (21)$$

where $\mathbf{w} \in \mathbb{R}^{N \times 3}$ is the matrix of unknown constant parameters to be estimated online, and $\epsilon_1(\mathbf{x}, \dot{\mathbf{x}})$ is the uniformly

bounded reconstruction error. The basis functions are the same as in the previous approximation. It can be seen that the function $\mathbf{a}(\mathbf{E}, \boldsymbol{\omega}, \tilde{\mathbf{E}}, \tilde{\boldsymbol{\omega}})$ is differentiable, therefore the mean value theorem can be applied [20] (p.108)

$$\mathbf{a}(\mathbf{E}, \boldsymbol{\omega}, \tilde{\mathbf{E}}, \tilde{\boldsymbol{\omega}}) = \mathbf{a}(\mathbf{E}_c, \boldsymbol{\omega}_c, \mathbf{0}, \mathbf{0}) + \nabla \mathbf{a}(\mathbf{E}_*, \boldsymbol{\omega}_*, \tilde{\mathbf{E}}_*, \tilde{\boldsymbol{\omega}}_*) \mathbf{z},$$

where $[\mathbf{E}_* \ \boldsymbol{\omega}_* \ \tilde{\mathbf{E}}_* \ \tilde{\boldsymbol{\omega}}_*] = \lambda[\mathbf{E} \ \boldsymbol{\omega} \ \tilde{\mathbf{E}} \ \tilde{\boldsymbol{\omega}}] + (1 - \lambda)[\mathbf{E}_c \ \boldsymbol{\omega}_c \ \mathbf{0} \ \mathbf{0}]$, $0 \leq \lambda \leq 1$ and $\mathbf{z} = [\tilde{\mathbf{E}} \ \tilde{\boldsymbol{\omega}} \ \tilde{\mathbf{E}} \ \tilde{\boldsymbol{\omega}}]^\top$. To be able to design implementable adaptive laws, we apply the universal approximation theorem to the continuous function $\bar{\mathbf{a}}(\mathbf{E}_c, \boldsymbol{\omega}_c) = B\mathbf{a}(\mathbf{E}_c, \boldsymbol{\omega}_c, \mathbf{0}, \mathbf{0})$, whereas the function $\tilde{\mathbf{a}} = \nabla \mathbf{a}(\mathbf{E}_*, \boldsymbol{\omega}_*, \tilde{\mathbf{E}}_*, \tilde{\boldsymbol{\omega}}_*) \mathbf{z}$ is dominated by a class \mathcal{K}_∞ function. That is, $\bar{\mathbf{a}}(\mathbf{E}_c, \boldsymbol{\omega}_c)$ is approximated over a compact domain $\Omega_E \times \Omega_\omega$ by a linear in parameters radial basis function (RBF) neural network [17]:

$$\bar{\mathbf{a}}(\mathbf{E}_c, \boldsymbol{\omega}_c) = W_2^\top \boldsymbol{\varphi}_2(\mathbf{E}_c, \boldsymbol{\omega}_c) + \boldsymbol{\epsilon}_2(\mathbf{E}_c, \boldsymbol{\omega}_c), \quad (22)$$

where $W_2 \in \mathbb{R}^{N \times 3}$ is the matrix of unknown constant parameters to be estimated online, and $\boldsymbol{\varphi}_2(\mathbf{E}_c, \boldsymbol{\omega}_c)$ is the vector of RBFs, and $\boldsymbol{\epsilon}_2(\mathbf{E}_c, \boldsymbol{\omega}_c)$ is the uniformly bounded reconstruction error. For the domination we recall Lemma 4.3 from [8] (p. 145) and show that there exist an increasing globally invertible function ρ such that

$$\|\nabla \mathbf{a}(\mathbf{E}_*, \boldsymbol{\omega}_*, \tilde{\mathbf{E}}_*, \tilde{\boldsymbol{\omega}}_*) \mathbf{z}\| \leq \rho(\|\boldsymbol{\xi}\|) \|\boldsymbol{\xi}\|, \quad (23)$$

where $\boldsymbol{\xi} = [\tilde{\mathbf{E}} \ \tilde{\boldsymbol{\omega}}]^\top$. The proof of this claim follows the steps of the upper bound in the above mentioned Lemma. The orientation error equation can now be written as follows

$$\begin{aligned} \dot{\tilde{\mathbf{E}}}(t) &= R(t)\tilde{\boldsymbol{\omega}}(t) - K_1\tilde{\mathbf{E}}(t) \\ \dot{\tilde{\boldsymbol{\omega}}}(t) &= \boldsymbol{\zeta}(t) - K_2\tilde{\boldsymbol{\omega}}(t) - R(t)\tilde{\mathbf{E}}(t) \\ B\dot{\boldsymbol{\zeta}}(t) &= \tilde{\boldsymbol{\delta}}(t) + W_1^\top \boldsymbol{\varphi}(x_c, \dot{x}_c) + W_2^\top \boldsymbol{\varphi}_2(\mathbf{E}_c, \boldsymbol{\omega}_c) \\ &\quad + \tilde{\mathbf{a}}(\boldsymbol{\xi}) + \boldsymbol{\sigma}(t), \end{aligned} \quad (24)$$

where uniformly bounded function $\boldsymbol{\sigma}(t)$ has the form

$$\begin{aligned} \boldsymbol{\sigma}(t) &= \mathbf{h}(t) + \boldsymbol{\epsilon}_1(x, \dot{x}) + \boldsymbol{\epsilon}_2(\mathbf{E}_c, \boldsymbol{\omega}_c) \\ &\quad + W_1^\top [\boldsymbol{\varphi}(x, \dot{x}) - \boldsymbol{\varphi}(x_c, \dot{x}_c)]. \end{aligned}$$

We define the control signal $\tilde{\boldsymbol{\delta}}(t)$ for the orientation error dynamics in (24) according to equation

$$\begin{aligned} \tilde{\boldsymbol{\delta}}(t) &= -\tilde{\boldsymbol{\omega}}(t) - K_3\boldsymbol{\zeta}(t) - \hat{W}_1^\top \boldsymbol{\varphi}(x_c, \dot{x}_c) \\ &\quad - \hat{W}_2^\top \boldsymbol{\varphi}_2(\mathbf{E}_c, \boldsymbol{\omega}_c) - \Upsilon(\tilde{\boldsymbol{\omega}})\hat{\boldsymbol{\sigma}}(t), \end{aligned} \quad (25)$$

where $K_3 > 0$ is the design parameter, \hat{W}_1 and \hat{W}_2 are the estimates of the unknown weight matrices W_1 and W_2 , $\hat{\boldsymbol{\sigma}}(t)$ is the estimate of the componentwise upper bound $\boldsymbol{\sigma}^*$ of the function $\boldsymbol{\sigma}(t)$, and $\Upsilon(\tilde{\boldsymbol{\omega}})$ is a diagonal matrix with the entries $\text{sign}(\tilde{\omega}_i)$, $i = 1, 2, 3$. The orientation control architecture is concluded by the adaptive laws for the estimates $\hat{\boldsymbol{\sigma}}(t)$, $\hat{W}_1(t)$ and $\hat{W}_2(t)$:

$$\begin{aligned} \dot{\hat{W}}_1(t) &= \Gamma_1 \boldsymbol{\varphi}(x_c, \dot{x}_c) \boldsymbol{\zeta}(t)^\top \\ \dot{\hat{W}}_2(t) &= \Gamma_2 \boldsymbol{\varphi}(\mathbf{E}_c, \boldsymbol{\omega}_c) \boldsymbol{\zeta}(t)^\top \\ \dot{\hat{\boldsymbol{\sigma}}}(t) &= \Gamma_3 \Upsilon(\tilde{\boldsymbol{\omega}}) \boldsymbol{\zeta}(t), \end{aligned} \quad (26)$$

The actual orientation control signal $\boldsymbol{\delta}(t)$ is the output of the stable low pass filter $G^{-1}(s) = (s\mathbb{I} + K_2)^{-1}$:

$$\boldsymbol{\delta}(t) = G^{-1}(s)\tilde{\boldsymbol{\delta}}(t). \quad (27)$$

The resulting orientation error dynamics have the form

$$\begin{aligned} \dot{\tilde{\mathbf{E}}}(t) &= R(t)\tilde{\boldsymbol{\omega}}(t) - K_1\tilde{\mathbf{E}}(t) \\ \dot{\tilde{\boldsymbol{\omega}}}(t) &= \boldsymbol{\zeta}(t) - K_2\tilde{\boldsymbol{\omega}}(t) - R(t)\tilde{\mathbf{E}}(t) \\ B\dot{\boldsymbol{\zeta}}(t) &= -\tilde{\boldsymbol{\omega}}(t) - K_3\boldsymbol{\zeta}(t) - \hat{W}_1^\top \boldsymbol{\varphi}(x_c, \dot{x}_c) + \tilde{\mathbf{a}}(\boldsymbol{\xi}) \\ &\quad - \hat{W}_2^\top \boldsymbol{\varphi}_2(\mathbf{E}_c, \boldsymbol{\omega}_c) - \Upsilon(\tilde{\boldsymbol{\omega}})\hat{\boldsymbol{\sigma}}(t) + \boldsymbol{\sigma}(t), \end{aligned} \quad (28)$$

IV. STABILITY ANALYSIS

In this section we proof the stability of the closed-loop system. The following technical lemma is needed for that purpose.

Lemma 1: For any $f \in C(R^+) \cap \mathcal{L}_\infty(R^+)$ and $D_\lambda(h) = \dot{h} + \lambda h \in L_\infty(R^+)$, $\lambda > 0$, there exist constants $c_1 > 0$ and c_2 such that

$$\int_0^t D_\lambda(h)(\tau) [c_1 \text{sign}(h(\tau)) - f(\tau)] d\tau \geq c_2. \quad (29)$$

Proof: All the functions involved in (29) are continuous, therefore integrable on any closed interval, except for the function $\text{sign}(h(\tau))$. From the hypothesis it follows that the number of proper local maxima of $h(\tau)$ on $[0, t]$ is at most countable [4]. This implies the set of discontinuities of $\text{sign}(h(\tau))$ is at most countable on $[0, t]$. Since $\text{sign}(h(\tau))$ is uniformly bounded, it follows from Lebesgue theorem [16] (p. 359) that $\text{sign}(h(\tau))$ is integrable on $[0, t]$. It is readily seen from the lemma's hypotheses that the function $h(\tau)$ is of bounded variation [9](p. 344). Therefore, there exists a constant $c_3 > 0$ such that

$$\left| \int_0^t f(\tau) d(h(\tau)) \right| \leq \alpha_u c_3. \quad (30)$$

where f_u is the upper bound for f . Using (30) we can derive the following lower bound for the integral in (29)

$$\begin{aligned} \int_0^t D_\lambda(h)(\tau) [c_1 \text{sign}(h(\tau)) - f(\tau)] d\tau &= c_1 \int_0^t d(|h(\tau)|) \\ &\quad + c_1 \lambda \int_0^t |h(\tau)| d\tau - \int_0^t f(\tau) d(h(\tau)) - \lambda \int_0^t f(\tau) h(\tau) d\tau \\ &\geq c_1 (|h(t)| - |h(0)|) + \lambda (c_1 - f_u) \int_0^t |h(\tau)| d\tau - f_u c_3. \end{aligned}$$

Choosing $c_1 \geq f_u$ results in (29), where $c_2 = -c_1|h(0)| - c_3 f_u$. The proof is complete. ■

Lemma 1 implies that the function $s(t) = c_2 - \int_0^t D_\lambda(h)(\tau) [f(\tau) - c_1 \text{sign}(h(\tau))] d\tau$ is nonnegative.

Theorem 1: Let the control signals $u(t)$ and $\boldsymbol{\delta}(t)$ be defined by the equations (17) and (27) respectively. Let the parameter estimates $\hat{\boldsymbol{\sigma}}_0(t)$, $\hat{\boldsymbol{w}}(t)$, $\hat{\boldsymbol{\sigma}}(t)$, $\hat{W}_1(t)$ and $\hat{W}_2(t)$ are defined according to adaptive laws in (16) and (26). Then, all signals in the closed loop system (18), (16), (28) and (26) are globally bounded. Moreover, the tracking and auxiliary errors $\tilde{V}(t)$, $\eta(t)$, $\tilde{\mathbf{E}}(t)$, $\tilde{\boldsymbol{\omega}}(t)$, and $\boldsymbol{\zeta}(t)$ converge to zero.

Proof: Define the candidate Lyapunov function:

$$\begin{aligned}
V &= \frac{1}{2} \left[\tilde{V}^2(t) + b\eta^2(t) + \tilde{\mathbf{E}}^\top(t) \tilde{\mathbf{E}}(t) + \tilde{\omega}^\top(t) \tilde{\omega}(t) \right] \\
&+ \frac{1}{2} \left[\zeta^\top(t) B \zeta(t) + \mu_0^{-1} \tilde{\sigma}_0^2(t) + \tilde{\mathbf{w}}^\top(t) \Gamma_0^{-1} \tilde{\mathbf{w}}(t) \right] \\
&+ \frac{1}{2} \text{tr} \left(\tilde{W}_1^\top(t) \Gamma_1^{-1} \tilde{W}_1(t) + \tilde{W}_2^\top(t) \Gamma_2^{-1} \tilde{W}_2(t) \right) \\
&+ \frac{1}{2} \left[\tilde{\sigma}^\top(t) \Gamma_3 \tilde{\sigma}(t) \right] + V_0(t), \quad (31)
\end{aligned}$$

where $\tilde{\sigma}_0(t) = \hat{\sigma}_0(t) - \sigma_0^*$ and $\tilde{\sigma}(t) = \hat{\sigma}(t) - \sigma^*$ are the corresponding upper bound estimation errors, and $\tilde{\mathbf{w}}(t) = \hat{\mathbf{w}}(t) - \mathbf{w}$, $\tilde{W}_1(t) = \hat{W}_1(t) - W_1$, $\tilde{W}_2(t) = \hat{W}_2(t) - W_2$ are the weight estimation errors. The time derivative of $V(t)$, computed along the trajectories of the systems in (18), (16), (28) and (26), after some algebra takes the form:

$$\begin{aligned}
\dot{V} &= \dot{V}_0 + \eta(t) \sigma_0(t) - k \tilde{V}^2(t) - c\eta^2(t) - \tilde{\mathbf{E}}^\top(t) K_1 \tilde{\mathbf{E}}(t) \\
&- \eta(t) \hat{\sigma}_0(t) \text{sign}(\tilde{V}) - \tilde{\omega}^\top(t) K_2 \tilde{\omega}(t) + \zeta^\top(t) \sigma(t) \\
&- \zeta^\top(t) K_3 \zeta(t) - \zeta^\top(t) \Upsilon(\tilde{\omega}) \hat{\sigma}(t) + \zeta^\top(t) \tilde{\alpha}(\xi).
\end{aligned}$$

Using the inequalities $|\sigma_0(t)| \leq \sigma_0^*$ and $\|\sigma(t)\| \leq \|\sigma^*\|$, the inequality in (23) and completing squares we can upper bound $\dot{V}(t)$ as follows:

$$\begin{aligned}
\dot{V} &= \sigma_0^{*2} - c_0[\tilde{\alpha}^2(t) + \tilde{\beta}^2(t)] - \left(\lambda_* - \frac{1}{4c_2^2} \rho^2(\xi) \right) \|\xi\|^2 \\
&- (k - c_1) \tilde{V}^2(t) - (c - 1) \eta^2(t) - c_3 \|\zeta(t)\|^2 + \|\sigma^*\|^2,
\end{aligned}$$

where $\lambda_{\min}(A)$ denotes the minimum eigenvalue of matrix A , $\lambda_* = \min\{\lambda_{\min}(K_1), \lambda_{\min}(K_2) - c_1\}$ and c_2 is chosen such that $c_3 = \lambda_{\min}(K_3) - c_2^2 > 0$. If we choose $c > 1$ and $k > c_1$, it follows that $\dot{V}(t) \leq 0$ when the following inequalities are satisfied

$$\begin{aligned}
k \tilde{V}^2 + (c - 1) \eta^2 &> \sigma_0^{*2}, \quad \|\zeta\| > \frac{\|\sigma^*\|}{\sqrt{\lambda_{\min}(K_3) - c_2^2}} \\
\|\xi\| &\leq \rho^{-1}(2c_* \sqrt{\lambda_*}). \quad (32)
\end{aligned}$$

implying the ultimate boundedness of the error signals $\tilde{\alpha}(t)$, $\tilde{\beta}(t)$, $\tilde{V}(t)$, $\eta(t)$, $\tilde{\mathbf{E}}(t)$, $\tilde{\omega}(t)$ and $\zeta(t)$. These in turn imply that the error signals $\dot{\tilde{V}}(t)$ and $\dot{\tilde{\omega}}(t)$ are bounded as well. To prove the asymptotic convergence we introduce the functions

$$\begin{aligned}
s_1(t) &= a_1 - \int_0^t \eta(\tau) \left[\sigma_0(\tau) - \sigma_0^* \text{sign}(\tilde{V}(\tau)) \right] d\tau \\
s_2(t) &= a_2 - \int_0^t \zeta^\top(\tau) \left[\sigma(\tau) - \Upsilon(\tilde{\omega}(\tau)) \sigma^* \right] d\tau, \quad (33)
\end{aligned}$$

where a_1 and a_2 are some constants. Since $\eta(t) = D_k(\tilde{V})(t)$, from Lemma 1 we conclude that $s_1(t)$ is nonnegative. The non-negativity of $s_2(t)$ does not follow directly from Lemma 1 because of the additional term $\int_0^t [\Upsilon(\tilde{\omega}(\tau)) \sigma^* - \sigma(\tau)]^\top R(\tau) \tilde{\mathbf{E}}(\tau) d\tau$, which appears after the substitution of $\zeta(t) = D_{K_2}(\tilde{\omega})(t) + R(t) \tilde{\mathbf{E}}(t)$. This additional term can be shown to be bounded below by noticing that from the orientation error dynamics $\dot{\tilde{\mathbf{E}}}(t) = K_1^{-1}(R(t) \tilde{\omega}(t) - \dot{\tilde{\mathbf{E}}}(t))$. The details are omitted here for the sake of brevity. Next, consider a new candidate Lyapunov function, defined in the variables $\tilde{\alpha}$, $\tilde{\beta}$, \tilde{V} , η , $\tilde{\mathbf{E}}$, $\tilde{\omega}$, ζ , $\tilde{\sigma}_0$, $\tilde{\mathbf{w}}$, \tilde{W}_1 , \tilde{W}_2 , $\tilde{\sigma}$, $\sqrt{s_1}$ and $\sqrt{s_2}$:

$$V_1(t) = V(t) + s_1(t) + s_2(t). \quad (34)$$

Similar to the previous case, it can be shown that the derivative of $V_1(t)$, computed along the trajectories of the systems in (18), (16), (28), (26) and (33), can be upper bounded as follows

$$\begin{aligned}
\dot{V}_1(t) &\leq -(k - c_1) \tilde{V}^2(t) - \left(\lambda_* - \frac{1}{4c_2^2} \rho^2(\xi) \right) \|\xi\|^2 \\
&- c_3 \|\zeta(t)\|^2 - c\eta^2(t) - c_0[\tilde{\alpha}^2(t) + \tilde{\beta}^2(t)],
\end{aligned}$$

which implies the semi-global boundedness of all error signals as long as the initial errors $\tilde{\mathbf{E}}(0)$ and $\tilde{\omega}(0)$ are chosen such that $\|\xi(0)\| \leq \rho^{-1}(2c_* \sqrt{\lambda_*})$. The boundedness of the states follows from the boundedness of the reference commands and their derivatives. Also, it follows that the parameter estimates $\hat{\sigma}_0(t)$, $\hat{\mathbf{w}}(t)$, $\hat{\sigma}(t)$, $\hat{W}_1(t)$, $\hat{W}_2(t)$ are bounded. As a result, the control signals $\tilde{u}(t)$ and $\tilde{\delta}(t)$ are bounded. Therefore, the error derivatives $\dot{\tilde{V}}(t)$, $\dot{\eta}(t)$, $\dot{\tilde{\mathbf{E}}}(t)$, $\dot{\tilde{\omega}}(t)$, and $\dot{\zeta}(t)$ are bounded, that is the error signals are uniformly continuous. Application of Barbalat's lemma ([22], p.19) results in $\tilde{V}(t) \rightarrow 0$, $\eta(t) \rightarrow 0$, $\tilde{\mathbf{E}}(t) \rightarrow 0$, $\tilde{\omega}(t) \rightarrow 0$, $\zeta(t) \rightarrow 0$ as $t \rightarrow \infty$. We also notice that the actual control signals $u(t)$ and $\delta(t)$ are bounded as the outputs of the stable low pass filters with bounded inputs. Since the states and their derivatives remain bounded, for any initial condition $\mathbf{x}(0)$ the compact set $\Omega_x \times \Omega_{\dot{x}}$ can be chosen such, the $\mathbf{x}(t) \in \Omega_x$ and $\dot{\mathbf{x}}(t) \in \Omega_{\dot{x}}$ for all $t \geq 0$, which validates the NN approximation in (14) and (21). The proof is complete. ■

V. SIMULATION RESULTS

For the simulation we use full nonlinear model of Sig Rascal 110 UAV from [7]. The external disturbances, which represent a variable wind gust, are set to $d_0(t) = \vartheta_1(t)$, $d_1(t) = 0.4 \sin(0.3t)$, $d_2(t) = \vartheta_2(t)$, $d_3(t) = 1.4 \sin(0.3t)$, where $\vartheta_1(t)$ is a square wave of amplitude 5 and of frequency 0.2rad/sec filtered trough a second order filter $G(s) = \frac{1}{s^2 + 3s + 1}$ and $\vartheta_2(t)$ is a square wave of amplitude 5 and of frequency 0.25rad/sec filtered trough a second order filter $G(s) = \frac{1}{s^2 + 3s + 1}$. The uncertainties in control effectiveness are set to $\lambda_T = 0.9$, $\Lambda = \text{diag}(0.9, 0.85, 0.85)$. The UAV is commanded to go from a straight climbing flight with velocity $V_0 = 65 \text{ ft/sec}$ and pitch angle of $\theta_0 = 10^\circ$ to a level flight with $V = 75 \text{ ft/sec}$ and pitch angle of $\theta = 0^\circ$ and to perform series of interchanging left and right coordinated turns following the corresponding left and right step commands of the amplitude of 15° . In order to provide the differentiability of the reference commands, a first order stable pre-filter with time constant 0.7 is used for the velocity channel, a second order stable filter $\frac{1}{s^2 + 2s + 1}$ is used for the pitch and yaw angle channels, and a second order stable filter $\frac{3}{s^2 + 4s + 3}$ is used in the bank angle channel. The tracking performance of the control algorithm is presented for a time interval of 60 sec. Figs. 1 and 3 display the tracking of the reference commands. It can be seen that the controller is capable of perfectly following the reference commands despite the uncertainties and disturbances. Figs. 2 and 4 show that Thrust and the control surface deflection commands are continuous and take on acceptable values.

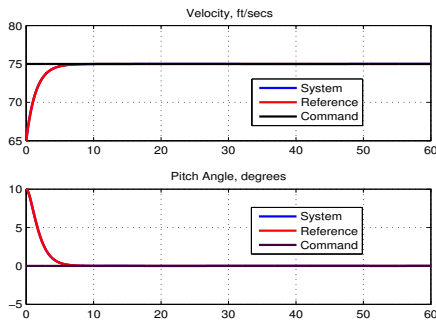


Fig. 1. Velocity and pitch angle tracking performance.

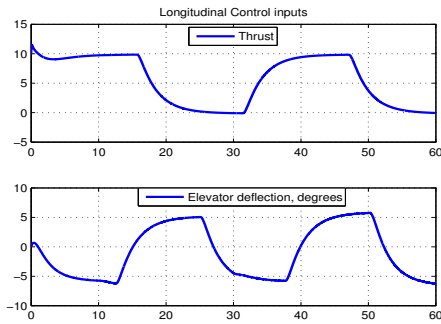


Fig. 2. Thrust and Elevator deflection commands.

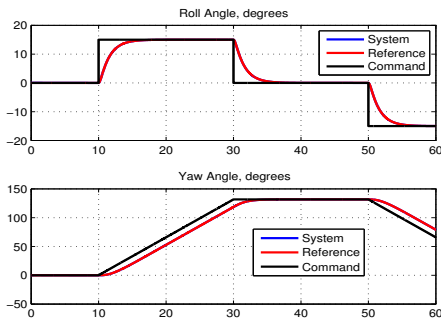


Fig. 3. Bank and yaw angle tracking performance.

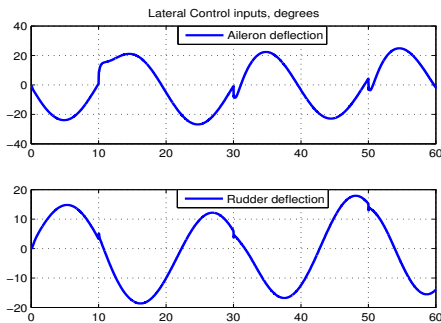


Fig. 4. Lateral control surface deflection commands.

VI. CONCLUSION

The paper presents a robust adaptive flight control methodology for the nonlinear UAVs to track smooth reference

commands. It is shown that the presented technique generates a continuous controller that guarantees asymptotic tracking without prior knowledge on the uncertainties, resulting from actuator failure or structural damages, and on the external disturbances. The performance of the proposed algorithm is demonstrated via numerical simulations.

REFERENCES

- [1] G. Bartolini, A. Ferrara, E. Usai, and V. Utkin. On Multi-Input Chattering-Free Second-Order Sliding Mode Control. *IEEE Trans. Autom. Contr.*, 45(9):1711–1717, September 2000.
- [2] F.C. Chen and C.C. Liu. Adaptively Controlling Nonlinear Continuous-time Systems Using Multilayer Neural Networks. *IEEE Trans. Autom. Contr.*, 39(6):1306–1310, 1994.
- [3] J.Y. Choi and J. Farrell. Observer-based Backstepping Control Using On-line Approximation. *Proc. of the American Control Conference*, pages 3646–3650, 2000.
- [4] V. Drobot and M. Morayne. Continuous Functions with a Dense Set of Proper Local Maxima. *The American Mathematical Monthly*, 92(3):209–211, March 1985.
- [5] J. A. Farrell and M. M. Polycarpou. *Adaptive Approximation Based Control: Unifying Neural, Fuzzy and Traditional Adaptive Approximation Approaches*. John Wiley, New York, 2006.
- [6] P.A. Ioannou and P.V. Kokotovic. Instability analysis and improvement of robustness of adaptive control. *Automatica*, 20(5):583–594, 1984.
- [7] N. M. Jodeh, P. A. Blue, and A. A. Waldron. Development of Small Unmanned Aerial Vehicle Research Platform: Modeling and Simulating with Flight Test Validations. In *Proc. of the AIAA Modeling and Simulation Technologies Conference and Exhibit, Keystone, Colorado, AIAA 2006-6261*, Aug. 21-24 2006.
- [8] H.K. Khalil. *Nonlinear Systems, Third Edition*. Prentice Hall, New Jersey, 2002.
- [9] A. N. Kolmogorov and S. V. Fomin. *Introductory Real Analysis*. Dover Publications, New York, 1975.
- [10] G. Kreisselmeier and B. Anderson. Robust Model Reference Adaptive Control. *IEEE Trans. Autom. Contr.*, AC-31(2):127–133, 1986.
- [11] M. Krstic, I. Kanellakopoulos, and P. Kokotovic. *Nonlinear and Adaptive Control Design*. John Wiley & Sons, New York, 1995.
- [12] Arie Levant. Universal Single-Input-Single-Output (SISO) Sliding-Mode Controllers With Finite-Time Convergence. *IEEE Trans. Autom. Contr.*, 46(9):1447–1451, September 2001.
- [13] F.L. Lewis, A. Yesildirek, and K. Liu. Multilayer Neural-Net Robot Controller with Guaranteed Tracking Performance. *IEEE Transactions on Neural Networks*, 7(2):1–12, 1996.
- [14] F.L. Lewis, A. Yesildirek, and K. Liu. Neural net Robot Controller: structure and Stability Proofs. *Journal of Intelligent and Robotic System*, 12:277–299, 1996.
- [15] K.S. Narendra and A.M. Annaswamy. A New Adaptive Law for Robust Adaptation Without Persistent Excitation. *IEEE Trans. Autom. Contr.*, 32(2):134–145, 1987.
- [16] S. M. Nikolsky. *A Course of Mathematical Analysis, Vol. 1*. MIR, Moscow (Translated from Russian by V. M. Volosov), 1975.
- [17] J. Park and I. Sandberg. Universal Approximation Using Radial Basis Function Networks. *Neural Computation*, 3:246–257, 1991.
- [18] M. M. Polycarpou. Stable Adaptive Neural Control Scheme for Nonlinear Systems. *IEEE Trans. Autom. Contr.*, 41(3):447–451, 1996.
- [19] J. B. Pomet and L. Praly. Adaptive Nonlinear Regulation: Estimation from the Lyapunov Equation. *IEEE Trans. Autom. Contr.*, 37(6):729–740, 1992.
- [20] W. Rudin. *Real and Abstract Analysis, 3rd ed.* McGraw-Hill, New York, 1986.
- [21] R. Sanner and J.J. Slotine. Gaussian Networks for Direct Adaptive Control. *IEEE Trans. Neural Networks*, 3(6):837–864, 1992.
- [22] S. S. Sastry and M. Bodson. *Adaptive Control: Stability, Convergence and Robustness*. Prentice Hall, 1989.
- [23] I. Shkolnikov and Y. Shtessel and M. D. J. Brown. A Second-Order Smooth Sliding Mode Control. In *Proceedings of IEEE Conference on Decision and Control, Orlando, FL*, pages 2803–2808, 2001.
- [24] B. L. Stevens and F. L. Lewis. *Aircraft Control and Simulation*. John Wiley & Sons, New York, 1992.
- [25] B. Xian, D.M. Dawson, M. S. Queiroz, and J. Chen. A Continuous Asiptotic Tracking Control Strategy for Uncertain Nonlinear Systems. *IEEE Trans. Autom. Contr.*, 49(7):1206–1211, July 2004.